# Analyst

Accepted Manuscript


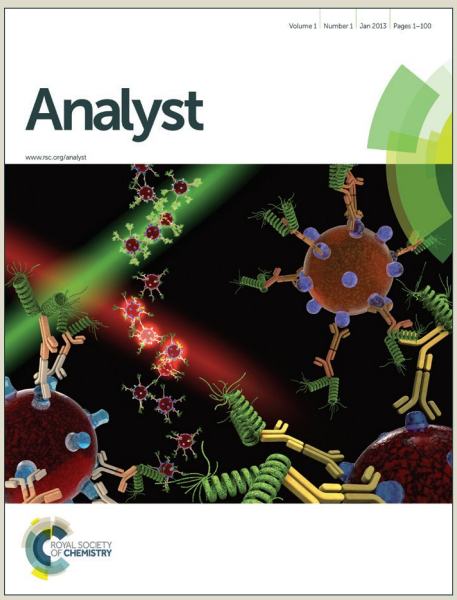



This is an *Accepted Manuscript*, which has been through the Royal Society of Chemistry peer review process and has been accepted for publication.

*Accepted Manuscripts* are published online shortly after acceptance, before technical editing, formatting and proof reading. Using this free service, authors can make their results available to the community, in citable form, before we publish the edited article. We will replace this *Accepted Manuscript* with the edited and formatted *Advance Article* as soon as it is available.

You can find more information about *Accepted Manuscripts* in the Information for Authors.

Please note that technical editing may introduce minor changes to the text and/or graphics, which may alter content. The journal's standard Terms & Conditions and the Ethical guidelines still apply. In no event shall the Royal Society of Chemistry be held responsible for any errors or omissions in this *Accepted Manuscript* or any consequences arising from the use of any information it contains.



ROYAL SOCIETY OF CHEMISTRY

www.rsc.org/analyst

# A turn-on fluorescent probe for hypochlorous acid based on the oxidation of diphenyl telluride

Parthiban Venkatesan, Shu-Pao Wu*

Analyst Accepted Manuscript

**Abstract**

A fluorescent probe, **HCTe** was developed for rapid detection of hypochlorous acid based on the specific HOCl-promoted oxidation of diphenyl telluride. The reaction is accompanied by a 82-fold increase in the fluorescent quantum yield (from 0.009 to 0.75). The fluorescent turn-on mechanism is achieved by suppression of the photo induced electron transfer (PET) from the diphenyl telluride group to BODIPY. The fluorescence intensity of the reaction between HOCl and **HCTe** is linear in the HOCl concentration range of 1 to 10 μM with a detection limit of 41.3 nM (S/N = 3). In addition, confocal fluorescence microscopy imaging using RAW264.7 macrophages demonstrated that **HCTe** could be an efficient fluorescent probe for HOCl detection in living cells.

Analyst Accepted Manuscript

## 1. Introduction

Hypochlorous acid (HOCl) is a reactive oxygen species (ROS), which has been used as a highly effective antimicrobial agent in mammalian immune systems.[1,2] Endogenous hypochlorite is formed from the reaction of hydrogen peroxide and chloride ions catalyzed by the heme-containing enzyme, myeloperoxidase (MPO) in leukocytes including macrophages, monocytes, and neutrophils.[3,4] However, excess production of hypochlorous acid in living organisms can cause various diseases, such as arthritis, cardiovascular disease, cancer, inflammatory disease and neuron degeneration.[5-7] Due to its biological importance, the development of highly sensitive and selective fluorescent probes will be useful in the dynamic detection of HOCl in living organisms.

The general approach for the design of HOCl fluorescent probes is to join a HOCl-reactive moiety with an organic fluorophore. HOCl has high oxidation properties. Several functional groups, such as p-alkoxyaniline, p-methoxyphenol, oxime, selenide, and thiol, have been identified as HOCl-reactive moieties.[8-24] The HOCl-reactive moiety functions as a controller that modulates the fluorescence intensity of the fluorophore. Organotellurium compounds are more electron rich than sulfur compounds, and have been used to design probes for some reactive oxygen species (ROS) and reactive nitrogen species (RNS).[25-27] Although several new HOCl sensors have been designed, fluorescent probes based on the redox cycle of tellurium to detect HOCl in living cells have not been studied in detail.

In this work, a new BODIPY (boron-dipyrromethene) based fluorescent probe **HCTe**, bearing an organotellurium group, was designed for HOCl detection (Scheme 1). The diphenyl telluride unit performed as a modulator that responds to the amount of HOCl, while BODIPY was used as the signal transduction unit. **HCTe** has weak fluorescence with a quantum yield of $\Phi$ = 0.009, due to the photoinduced electron transfer (PET) from the diphenyl telluride group to the BODIPY moiety. However, the strong fluorescence of BODIPY is restored after the oxidation of tellurium by HOCl. This new probe exhibits higher selectivity and sensitivity towards HOCl in aqueous solutions, compared to other ROS and reactive nitrogen species (RNS). Most importantly, **HCTe** shows good cell-membrane permeability and can be successfully applied to image endogenous HOCl in living cells.

## 2. Materials and methods

### 2.1 Materials and Instrumentation

All solvents and reagents were obtained from commercial sources and used without further purification. UV/Vis spectra were recorded on an Agilent 8453 UV/Vis spectrometer. Fluorescence spectra measurements were performed on a Hitachi F-7000 fluorescence spectrophotometer. NMR spectra were obtained on a Bruker

Analyst Accepted Manuscript

DRX-300 and Agilent Unity INOVA-500 NMR spectrometer. Fluorescent images were taken on a Leica TCS SP5 X AOBS Confocal Fluorescence Microscope.

**2.2 Preparation of ROS and RNS:**

Various ROS and RNS including HOCl, $^{\bullet}OH$, $H_2O_2$, $^1O_2$, $NO_2^-$, $NO_3^-$, NO, $ONOO^-$, $O_2$, and *t*-BuOOH were prepared according to the following methods. HOCl was prepared from commercial bleach; the concentration of hypochlorite ($OCl^-$) was determined by using an extinction coefficient of 350 $M^{-1}cm^{-1}$ (292 nm) at pH 9.0. Hydroxyl radical ($^{\bullet}OH$) was generated by Fenton reaction on mixing $Fe(NH_4)_2(SO_4)_2 \cdot 6H_2O$ with 10 equivalents of $H_2O_2$; the concentration of $^{\bullet}OH$ was estimated from the concentration of $Fe^{2+}$. The concentration of the commercially available stock $H_2O_2$ solution was estimated by optical absorbance at 240 nm. Singlet oxygen ($^1O_2$) was generated by the addition of NaOCl and $H_2O_2$ according to the literature.[28] The source of $NO_2^-$ and $NO_3^-$ was from $NaNO_2$ and $NaNO_3$. Nitric oxide (NO) was generated from sodium nitroferricyanide(III) dihydrate. Peroxynitrite ($ONOO^-$) was prepared as the reported method;[29] the concentration of peroxynitrite was estimated by using an extinction coefficient of 1670 $M^{-1}cm^{-1}$ (302 nm). Superoxide ($O_2^-$) is prepared from $KO_2$. *t*-BuOOH was obtained commercially from Alfa Aesar.

**2.3 Synthesis of 2-(phenyltellanyl) benzaldehyde:**

To a mixture of CuI (11.59 mg, 0.05mmol) and 2,2'- dipyridyl (9.56 mg, 0.05 mmol) in DMSO (1 mL) and $H_2O$ (1 mL), biphenyl ditelluride (500 mg, 1.22 mmol) and 2-formyl phenyl boronic acid (546 mg, 3.66 mmol) were added. The reaction mixture was stirred at 100°C for 5 hr in air. The reaction mixture was diluted with water and extracted with dichloromethane. The combined organic layer was dried over anhydrous $MgSO_4$ and the solvent was removed under reduced pressure. The crude product was purified by column chromatography (hexane: dichloromethane = 1:1) to give the compound as a yellow oil. Yield: 300 mg (55%). $^1H$ NMR (300 MHz, $CDCl_3$): $\delta$ 9.91 (s, 1H), 7.85 (d, $J$ = 7.2 Hz, 2H), 7.63 (m, 4H), 7.39 (t, $J$ = 6.6 Hz, 1H), 7.31 (t, $J$ = 7.5 Hz, 2H); $^{13}C$ NMR (75 MHz, $CDCl_3$): $\delta$ 191.7, 140.0, 138.0, 135.7, 135.2, 130.0, 129.1, 127.0, 113.2. MS ($ESI^+$): $m/z$ = 312.9 $[M + H]^+$; HRMS ($ESI^+$): Calcd. for $C_{13}H_{10}OTe$, 312.9872 $[M + H]^+$; found, 312.9862 $[M + H]^+$. FTIR ($cm^{-1}$) 3050, 2812, 1659, 1580, 1552, 1450, 1432, 1383, 1300, 1255, 1210, 1114, 1018, 845, 740, 695.

**2.4 Synthesis procedure of HCTe**

TFA (0.1 mL) was added to the solution of 2-(phenyltellanyl)benzaldehyde (300 mg, 0.682 mmol) and ,2,4-dimethylpyrrole (136.40 mg, 1.433 mmol) in $CH_2Cl_2$

Analyst Accepted Manuscript

(100 mL) under $N_2$ atmosphere. After the solution was stirred for 6 h, TLC analysis revealed complete conversion of starting materials to the dipyrromethane. To the reaction mixture, DDQ (170 mg, 0.7502 mmol) dissolved in $CH_2Cl_2$ (50 mL) was added. Then, the solution was stirred for further 1h; TLC analysis revealed the complete disappearance of dipyrromethane and formation of the desired dipyrromethene. Triethyl amine (4.0 mL) and $BF_3.Et_2O$ (4.0 mL) were added to the reaction mixture and stirring was continued for further 5 h. Reaction mixture was washed with water (50 mL) by three times and the organic phase was dried over anhydrous $MgSO_4$. The solvent was removed under reduced pressure and the crude product was purified by column chromatography (hexane : dichloromethane = 1:1) to give the compound **HCTe** as a red solid. Yield: 290 mg (80 %); melting point 129-130 $^0$C. $^1$H NMR (300 MHz, $CDCl_3$): $\delta$ 7.86 (d, $J$ = 6.9 Hz, 2H), 7.42-7.18 (m, 7H), 6.01 (s, 2H), 2.61 (s, 6H), 1.50 (s, 6H); $^{13}$C NMR (75 MHz, $CDCl_3$) δ 156.2, 142.7, 141.9, 141.5, 141.3, 138.4, 135.4, 130.7, 129.7, 129.0, 128.2, 127.9, 121.4, 119.6, 112.5,14.8,14.3; $^{125}$Te NMR (158 MHz, $CDCl_3$): $\delta$ 665.6. MS ($ESI^+$): $m/z$ = 531.0 $[M + H]^+$; HRMS ($ESI^+$): calcd. for $C_{25}H_{23}BF_2N_2Te$, 531.1062 $[M + H]^+$, found, 531.1057 $[M + H]^+$. FTIR ($cm^{-1}$) 3055, 2918, 1544, 1506, 1308, 1196, 1148, 1086, 984, 740, 700.

**2.5 The oxidized product (HCTeO) from the reaction of HCTe and NaOCl**

NaOCl (0.3 mL, 12% dissolved in $H_2O$) was added to the solution of HCTe (60 mg) in $CH_3OH$ (50 mL). The reaction mixture was stirred at room temperature for 30 min. The solvent was evaporated under reduced pressure and the crude product was purified by column chromatography (Ethyl acetate / $CH_3OH$ = 9 : 1) to give the compound HCTeO as a dark red powder. Yield: 40 mg. (65%); melting point, 165-166$^0$C. $^1$H NMR (500 MHz, $CDCl_3$): $\delta$ 8.09 (d, $J$ = 7.5Hz, 2H), 7.52 (td, $J$ = 7.5, 1.0 Hz, 1H), 7.39 (td, $J$ = 8.5, 1.0 Hz, 1H), 7.25 (s,1H), 7.15-7.11 (m, 2H), 7.01 (t, $J$ = 7.0 Hz, 2H), 5.98 (s, 2H), 2.53 (s, 6H), 1.35 (s, 6H); $^{13}$C NMR (75 MHz, $CDCl_3$) δ 157.1, 156.9, 143.8, 142.7, 137.9, 137.6, 137.3, 136.6, 131.1, 130.8, 130.5, 130.4, 130.2, 130.1, 129.0, 128.5, 122.2, 121.8, 14.5, 13.8. $^{125}$Te NMR (158MHz, $CDCl_3$): $\delta$ 1113.6. MS (ESI+): $m/z$ = 547.1 $[M + H]^+$; HRMS ($ESI^+$): Calcd. for $C_{25}H_{23}BF_2N_2TeO$, 547.1012 $[M + H]^+$, found 547.1001 $[M + H]^+$. FTIR ($cm^{-1}$) 3042, 2965, 1542, 1514, 1423, 1315, 1194, 1156, 1085, 977, 743, 734, 700.

**2.6 Cell culture for RAW264.7 Macrophages**

The cell line RAW264.7 was provided by the Food Industry Research and Development Institute (Taiwan). RAW264.7 cells were cultured in Dulbecco's modied Eagle's medium (DMEM) supplemented with 10% fetal bovine serum (FBS) at 37 °C under an atmosphere of 5% $CO_2$. Cells were plated on 18 mm glass coverslips and

Analyst Accepted Manuscript

allowed to adhere for 24 h.

**2.7 Cytotoxicity assay**

The methyl thiazolyl tetrazolium (MTT) assay was used to measure the cytotoxicity of **HCTe** in RAW264.7 cells. RAW264.7 cells were seeded into a 96-well cell-culture plate. Various concentrations (5, 10, 15, 20, 25 μM) of **HCTe** were added to the wells. The cells were incubated at 37 ° C under 5% $CO_2$ for 24 h. 10 μL MTT (5 mg/mL) was added to each well and incubated at 37 ° C under 5% $CO_2$ for 4 h. Remove the MTT solution and yellow precipitates (formazan) observed in plates were dissolved in 200 μL DMSO and 25 μL Sorenson's glycine buffer (0.1 M glycine and 0.1 M NaCl). Multiskan GO microplate reader was used to measure the absorbance at 570 nm for each well. The viability of cells was calculated according to the following equation:

Cell viability (%) = (mean of absorbance value of treatment group) / (mean of absorbance value of control group).

**2.8 Fluorescence imaging of Exogenous HCTe in Living Cells**

Experiments to assess the sensing ability of **HCTe** for exogenous HOCl were performed in 0.1 M phosphate-buffered saline (PBS) with NaOCl (10 μM). Treat the cells with 2 μL of 10 mM **HCTe** (final concentration: 10 μM) dissolved in DMSO and incubated for 30 min at 37 ℃. The treated cells were washed with 0.1 M PBS (2 mL × 3) to remove remaining **HCTe**. DMEM (2 mL) was added to the cell culture, which was then treated with 10 mM solution of NaOCl (2 μL; final concentration: 10 μM) dissolved in sterilized 0.1 M PBS (pH 7.4). The samples were incubated at 37 ° C for 10 min. The culture medium was removed, and the treated cells were washed with 0.1 M PBS (2 mL × 3) before observation. Confocal fluorescence imaging of cells was performed with a Leica TCS SP5 X AOBS Confocal Fluorescence Microscope (Germany), and a 63x oil-immersion objective lens was used. The cells were excited with a white light laser at 488 nm, and emission was collected at 530 ±10 nm.

**2.9 Fluorescence Imaging of PMA-Induced HOCl Production in Living Cells**

RAW264.7 cells were treated with PMA (25 ng/mL) and **HCTe** in culture medium for 2 h. The culture medium was removed, and the treated cells were washed with 0.1 M PBS (2 mL × 3) before observation. Fluorescence imaging was performed with a Leica TCS SP5 X AOBS Confocal Fluorescence Microscope. The cells were excited with a white light laser at 488 nm, and emission was collected at 530 ±10 nm.

Analyst Accepted Manuscript

### 2.10 Quantum chemical calculation

Quantum chemical calculations based on density functional theory (DFT) were carried out using a Gaussian 09 program. The optimized geometries and energy levels of frontier molecular orbitals were performed using the B3LYP functional and the 6-31G basis set.

## 3. Results and discussion

### 3.1 Synthesis of the probe HCTe

The synthesis of the probe **HCTe** is outlined in Scheme 1. 2-(Phenyltellanyl) benzaldehyde was first prepared from the reaction of biphenyl ditelluride with 2-formyl phenyl boronic acid in the presence of CuI and 2,2'-dipyridyl. Treatment of 2-(phenyltellanyl) benzaldehyde with 2,4-dimethylpyrrole in the presence of trifluoroacetic acid (TFA) under $N_2$ produces the corresponding dipyrromethane. The dipyrromethane is then oxidized with 2,3-dichloro-5,6-dicyano-1,4-benzoquinone (DDQ) to produce the corresponding dipyrromethene, which is transformed into the BODIPY skeleton in the presence of $BF_3$. The structures of **HCTe** and **HCTeO**, the product of the reaction of **HCTe** with HOCl, were confirmed using $^1H$ and $^{13}C$ NMR spectroscopy and mass spectrometry.

### 3.2 Fluorescent response of HCTe with HOCl

We tested the sensing performance of the probe **HCTe** towards various ROS and RNS species, including HOCl, $^{\bullet}OH$, $H_2O_2$, $^1O_2$, $NO_2^-$, $NO_3^-$, NO, $ONOO^-$, $O_2$, and *t*-BuOOH, in a phosphate-buffered saline (PBS) solution. We found that strong green fluorescence only occurred upon addition of HOCl to a solution containing **HCTe**; other ROS and RNS produced no change in fluorescence (Fig. 1). Quantitative **HCTe** fluorescence was observed in the presence of several ROS and RNS that were tested, however, HOCl was the only reactive species that enhanced the fluorescence significantly. To study the influence of other ROS/RNS on the reaction of **HCTe** with HOCl, competitive experiments were performed with other ROS/RNS (100 μM) in the presence of NaOCl (20 μM).

In Fig. 2, the fluorescence enhancement caused by mixing NaOCl with most ROS/RNS was similar to that caused by NaOCl alone. When NaOCl was mixed with $H_2O_2$, the fluorescence intensity was lower. NaOCl reacts with $H_2O_2$ to produce $^1O_2$, which does not respond to the **HCTe** probe. Due to the consumption of NaOCl by $H_2O_2$, a lower fluorescence intensity was observed in the presence of NaOCl and $H_2O_2$.[28] To further evaluate the selectivity of the **HCTe** probe towards HOCl, 15 different metal ions ($Ag^+$, $Al^{3+}$, $Ca^{2+}$, $Cd^{2+}$, $Co^{2+}$, $Cr^{3+}$, $Cu^{2+}$, $Fe^{2+}$, $Fe^{3+}$, $Hg^{2+}$, $Mg^{2+}$,

Analyst Accepted Manuscript

$Mn^{2+}$, $Ni^{2+}$, $Pb^{2+}$, $Zn^{2+}$) and 10 different anions ($Br^-$, $CH_3COO^-$, $CN^-$, $F^-$, $HSO_4^-$, $HPO_4^{2-}$, $H_2PO_4^-$, $I^-$, $OH^-$, $SCN^-$) were tested. None of the ions tested produced a noticeable change in fluorescence intensity (Figure S17 and Figure S18 in the supporting information), indicating no response toward the **HCTe** probe. These results suggest that **HCTe** may respond to HOCl with low interference.

The reaction of **HCTe** with HOCl is fast; addition of NaOCl(aq) to a solution containing **HCTe** results in an immediate, strong increase in fluorescence intensity (see Figure S19 in the supporting information). During the titration of HOCl with **HCTe**, a new emission band appeared at 531 nm (Fig. 3). The emission intensity reached its maximum after the addition of one equivalent of HOCl. The quantum yield of the oxidized form, **HCTe**, was $\Phi = 0.75$, which is 82-fold greater than that of **HCTe** (0.009). The structure of **HCTeO** was confirmed by $^1$H NMR, $^{13}$C NMR, and MS spectrometry. We observed a good linear correlation between fluorescence intensity and HOCl concentration over the range of 0–10 μM, and found that **HCTe** has a detection limit of 41.3 nM (Figure S20 in the Supporting Information), indicating that it is sufficiently sensitive for the detection of HOCl in living cells.

The HOCl-detection mechanism was determined by the density functional theory (DFT) calculation. As shown in Scheme 2, the highest occupied molecular orbital (HOMO) of the diphenyl telluride moiety (electron donor) is close to that of the fluorophore BODIPY (electron acceptor); the HOMO energy level (−5.45 eV) of the diphenyl telluride moiety is higher than that of BODIPY (−5.57 eV). Consequently, when the BODIPY moiety is excited by light, the electron transfer from the diphenyl telluride moiety to the BODIPY moiety is energetically allowed.Hence, the BODIPY fluorescence is quenched by the PET process ($\Phi < 0.01$). In contrast, upon the oxidation of **HCTe** by HOCl, the HOMO energy level of the diphenyl telluroxide moiety (−6.29 eV) is below that of BODIPY. Thus, the PET process is avoided and the fluorescence of BODIPY is restored.[30]

An experiment was conducted to determine the pH-dependence of **HCTe**, to establish a suitable pH range for HOCl sensing. Figure 4a shows that the emission intensities of **HCTe** are very low at a pH range of 4 – 10. After the addition of one equivalent of HOCl, the emission intensity at 531 nm increases significantly at a pH range of 5.5 – 8.0, which means that the probe could be used under these physiological conditions. When the pH exceeded 8.0, the emission intensity dropped slightly. This is because the p$K_a$ of HOCl is 7.6 and hypochlorite ($ClO^-$), which is dominant at pH > 8, has slightly poor reactivity with **HCTe**. The reducing agent glutathione (GSH) was used to determine the ability of **HCTeO** to be reduced to its original state. Figure 4b shows the reaction of the oxidized product **HCTeO** with GSH. A remarkable decrease in fluorescence was observed after the addition of GSH.

Analyst Accepted Manuscript

This observation indicates the reversibility of **HCTe**, which can be used to monitor the dynamic changes in the HOCl present in living cells.

### 3.3 Bioimaging of HCTe

The potential of the probe **HCTe** for imaging HOCl in living cells was also investigated. RAW264.7 macrophages were used as a model cell line because macrophages are known to generate ROS and RNS in the immune system. An MTT assay was conducted with a RAW264.7 cell line to evaluate the cytotoxicity of **HCTe**. The cellular viability was estimated to be greater than 80% after 24 h, which indicates that **HCTe** (<25 μM) has low cytotoxicity (see Figure S21 in the supporting information). Images of cells were obtained using confocal fluorescence microscopy. No fluorescence was observed for RAW264.7 cells that were incubated with 10 μM **HCTe** (Fig. 5a). After treatment with NaOCl, bright green fluorescence was observed in the RAW264.7 cells (Fig. 5b). The overlay of fluorescence and bright-field images revealed that the fluorescence signals were localized in the intracellular area, indicating a subcellular distribution of HOCl and good cell-membrane permeability of **HCTe**. Further addition of GSH (200 μM) in the culture medium caused the intracellular fluorescence in RAW264.7 cells to disappear (Figure 5c). This indicates that the oxidized probe (**HCTeO**) was reduced to the nonfluorescent probe (**HCTe)** by GSH.

Furthermore, **HCTe** was used to detect PMA-induced endogenous HOCl production in RAW264.7 cells. Phorbol myristate acetate (PMA) activates the generation of ROS and RNS, including HOCl, in macrophage cells.[31,32] After stimulation with PMA (25 ng/mL) for 2 h in the presence of **HCTe**, strong green fluorescence was observed in the RAW264.7 cells (Fig. 6a). These results demonstrate that **HCTe** can enable the visualization of PMA-induced endogenous HOCl production in macrophages. When the MPO inhibitor 4-aminobenzoic acid hydrazide (ABAH, 100 μM) was added to macrophage cells with PMA (25ng/mL), no fluorescence enhancement was observed. These results demonstrate that the presence of HOCl results in significant fluorescence enhancement in cells, whereas the fluorescence enhancement produced by other ROS and RNS is negligible.

## 4. Conclusion

In summary, we have developed a BODIPY-based green fluorescent probe, **HCTe**, which displays a rapid, highly selective, and sensitive response to HOCl over other reactive species. This system utilizes the HOCl-promoted oxidation of diphenyl telluride to respond to the amount of HOCl. **HCTe** is rapidly oxidized by HOCl with an increase in emission. Confocal fluorescence microscopy imaging using RAW264.7 cells showed that the probe **HCTe** could be used to evaluate the role of HOCl in biological systems

Analyst Accepted Manuscript

**Acknowledgements**

We gratefully acknowledge the financial support of Ministry of Science and Technology (Taiwan, 101-2113-M-009-016-MY2) and National Chiao Tung University.

**Notes and references**

*Department of Applied Chemistry, National Chiao Tung University, Hsinchu, Taiwan 300, ROC. E-mail: spwu@mail.nctu.edu.tw; Tel: +886-3-5712121 ext. 56506*

*Electronic supplementary information (ESI) available:* $^{1}$H and $^{13}$C NMR spectra of **HCTe**, ESI-Mass of **HCTe** and **HCTeO**, calibration curve of **HCTe**–NaOCl in a water-$CH_3OH$ solution, cell viability values estimated by an MTT assay

**References**

1 C. C. Winterbourn, M. B. Hampton, J. H. Livesey and A. J. Kettle, *J. Biol. Chem*., 2006, **281**, 39860-39869.

2 X. Chen, X. Tian, I. Shin and J. Yoon, *Chem. Soc. Rev.*, 2011, **40**, 4783-4804.

3 T. J. Fiedler, C. A. Davey and R. E. Fenna, *J. Biol. Chem.*, 2000, **275**, 11964-11971.

4 Y. W. Yap, M. Whiteman and N. S. Cheung, *Cell. Signal.,* 2007, **19**, 219-228.

5 L. J. Hazell, L. Arnold, D. Flowers, G. Waeg, E. Malle and R. Stocker, *J. Clin. Invest.*, 1996, **97**, 1535-1544.

6 V. Rudolph, R. P. Andrie, T. K. Rudolph, K. Friedrichs, A. Klinke, B. Hirsch-Hoffmann, A. P. Schwoerer, D. Lau, X. Fu, K.Klingel, K. Sydow, M. Didie, A. Seniuk, E.-C. von Leitner, K. Szoecs, J. W. Schrickel, H. Treede, U. Wenzel, T. Lewalter, G. Nickenig, W.-H. Zimmermann, T. Meinertz, R. H. Boger, H. Reichenspurner, B. A. Freeman, T. Eschenhagen, H. Ehmke, S. L. Hazen, S. Willems and S. Baldus, *Nat. Med.*, 2010, **16**, 470-474.

7 M. Whiteman, P. Rose, J. L. Siau, N. S. Cheung, G. S. Tan, B. Halliwell and J. S. Armstrong, *Free Radic. Biol. Med.*, 2005, **38**, 1571-1584.

8 Z.-N. Sun, F.-Q. Liu, Y. Chen, P. K. H. Tam and D. Yang, *Org. Lett.*, 2008, **10**, 2171-2174.

9 Y.-K. Yang, H. J. Cho, J. Lee, I. Shin and J. Tae, *Org. Lett.*, 2009, **11**, 859-861.

Analyst Accepted Manuscript

10 Y. Koide, Y. Urano, K. Hanaoka, T. Terai and T. Nagano, *J. Am. Chem. Soc.*, 2011, **133**, 5680-5682.
11 X. Cheng, H. Jia, T. Long, J. Feng, J. Qin and Z. Li, *Chem. Commun.*, 2011, **47**, 11978-11980.
12 L. Yuan, W. Lin, J. Song and Y. Yang, *Chem. Commun.*, 2011, **47**, 12691-12693.
13 Y. Zhou, J.-Y. Li, K.-H. Chu, K. Liu, C. Yao and J.-Y. Li, *Chem. Commun.*, 2012, **48**, 4677-.4679
14 B. Wang, P. Li, F. Yu, P. Song, X. Sun, S. Yang, Z. Lou and K. Han, *Chem. Commun.*, 2013, **49**, 1014-1016.
15 S.-R. Liu and S.-P. Wu, *Org. Lett.*, 2013, **15**, 878-881.
16 S.-R. Liu, M. Vedamalai and S.-P. Wu, *Anal. Chim. Acta.*, 2013, **800**, 71-76.
17 Q. Xu, K.-A. Lee, S. Lee, K. M. Lee, W.-J. Lee and J. Yoon, *J. Am. Chem. Soc.*, 2013, **135**, 9944-9949.
18 M. Emrullahoglu, M. Ucuncu and E. Karakus, *Chem. Commun.*, 2013, **49**, 7836-7838.
19 G. Cheng, J. Fan, W. Sun, J. Cao, C. Hu and X. Peng, *Chem. Commun.*, 2014, **50**, 1018-1020.
20 J. J. Hu, N.-K. Wong, Q. Gu, X. Bai, S. Ye and D. Yang, *Org. Lett.*, 2014, **16**, 3544-3547.
21 S. Yu, C. Hsu, W. Chen, L. Wei, S. Wu, *Sens. Actuators B*, 2014, **196**, 203-207.
22 J. Li, F. Huo and C. Yin, *RSC Advances*, 2014, **4**, 44610–44613.
23 F. Liu, Y. Gao, J. Wang and S. Sun, *Analyst*, 2014, **139**, 3324–3329.
24 J. Kim and Y. Kim, *Analyst*, 2014, **139**, 2986–2989.
25 S. T. Manjare, J. Kim, Y. Lee and D. G. Churchill, *Org. Lett.*, 2013, **16**, 520-523.
26 L. A. Ba, M. Doring, V. Jamier and C. Jacob, *Org. Biomol. Chem.*, 2010, **8**, 4203-4216.
27 F. Yu, P. Li, B. Wang and K. Han, *J. Am. Chem. Soc.*, 2013, **135**, 7674-7680.
28 X. Li, G. Zhang, H. Ma, D. Zhang, J. Li and D. Zhu, *J. Am. Chem. Soc.*, 2004, **126**, 11543-11548.
29 J. W. Reed, H. H. Ho and W. L. Jolly, *J. Am. Chem. Soc.*, 1974, **96**, 1248-1249.
30 A. Loudet and K. Burgess, *Chem. Rev.*, 2007, **107**, 4891-4932.

Analyst Accepted Manuscript

31 M. Wolfson, L. C. McPhail, V. N. Nasrallah and R. Snyderman, J. Immunol., 1985, **135**, 2057-2062.

32 Y.-C. Yang, H.-H. Lu, W.-T. Wang and I. Liau, *Anal. Chem.*, 2011, **83**, 8267-8272.

Analyst Accepted Manuscript

**Scheme and Figure Captions:**

1. **Scheme 1**. Synthesis of **HCTe**

2. **Scheme 2.** Energy level diagram for the reaction of **HCTe** with **HOCl**.

3. **Fig. 1.** Fluorescence response of **HCTe** (10 μM) toward HOCl and other ROS and RNS (100 μM) in $H_2O$-$CH_3OH$ (v/v = 99/1, 0.1 M PBS, pH 7.4). The excitation wavelength was 480 nm.

4. Fig 2. Fluorescence changes (530 nm) of probe HCTe (10 μM) to NaOCl (15 μM) or 100 μM of other ROS/RNS (the black bar portion) and to the mixture of other ROS/RNS (100 μM) with 15 μM of NaOCl (the red bar portion) in a water– $CH_3OH$ solution (v/v = 99/1, 0.1 M PBS, pH 7.4). The excitation wavelength was 480 nm.

5. Fig. 3. Fluorescence changes of **HCTe** (10 μM) in the presence of various equivalents of NaOCl in a $H_2O$-$CH_3OH$ (v/v = 99/1, 0.1 M PBS, pH 7.4) solution. The excitation wavelength was 480 nm.

6. **Fig. 4.** (top) Fluorescence response (530 nm) of free probe **HCTe** (10 μM), and after addition of NaOCl (10 μM) to a $H_2O$–$CH_3OH$ solution (v/v = 99/1) different pH values. (bottom) Reversibility of the interaction between **HCTe** (10 μM) and NaOCl (10 μM) by the introduction of GSH to the system in a $H_2O$-$CH_3OH$ (v/v = 99/1, 0.1 M PBS, pH 7.4) solution.

7. **Fig. 5**. Fluorescence images of RAW264.7 cells. (Left) Bright field image; (Middle) fluorescence image; and (Right) merged image. (a) The cells incubated with **HCTe** (10 μM) for 30 min. (b) Subsequent treatment of the cells with NaOCl (10 μM) for 10 min. (c) Further incubation with GSH (200 μM) for 30 min.

8. **Fig. 6.** Detection of PMA-induced HOCl production in RAW264.7 cells. (a) The cells treated with PMA (25 ng/mL) for 2 h at 37 °C in the presence of **HCTe** (10 μM). (b) ABAH (100 μM) was co-incubated with **HCTe** (10 μM) for 1 h at 37 °C during PMA stimulation.

Analyst Accepted Manuscript

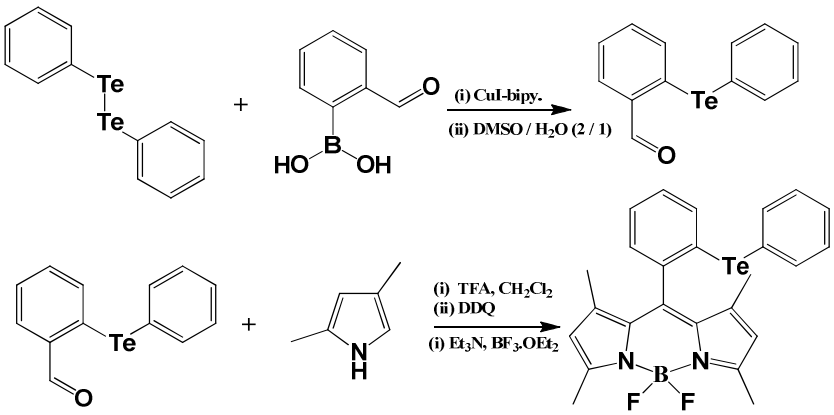


**Scheme 1**. Synthesis of **HCTe**

Analyst Accepted Manuscript

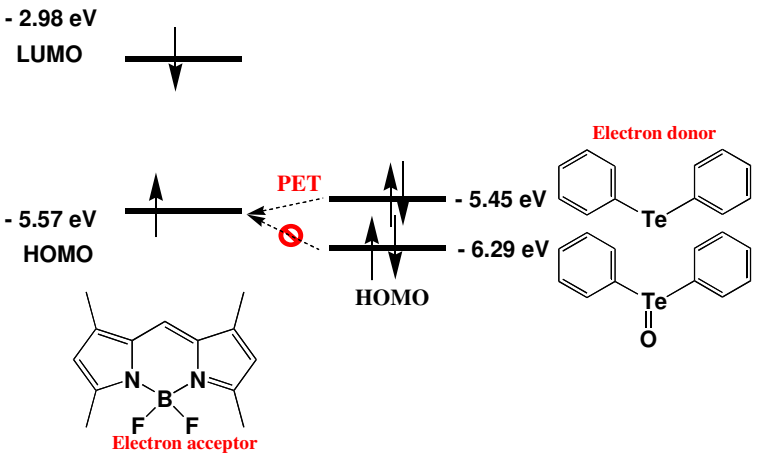


**Scheme 2.** Energy level diagram for the reaction of **HCTe** with **HOCl**.

Analyst Accepted Manuscript

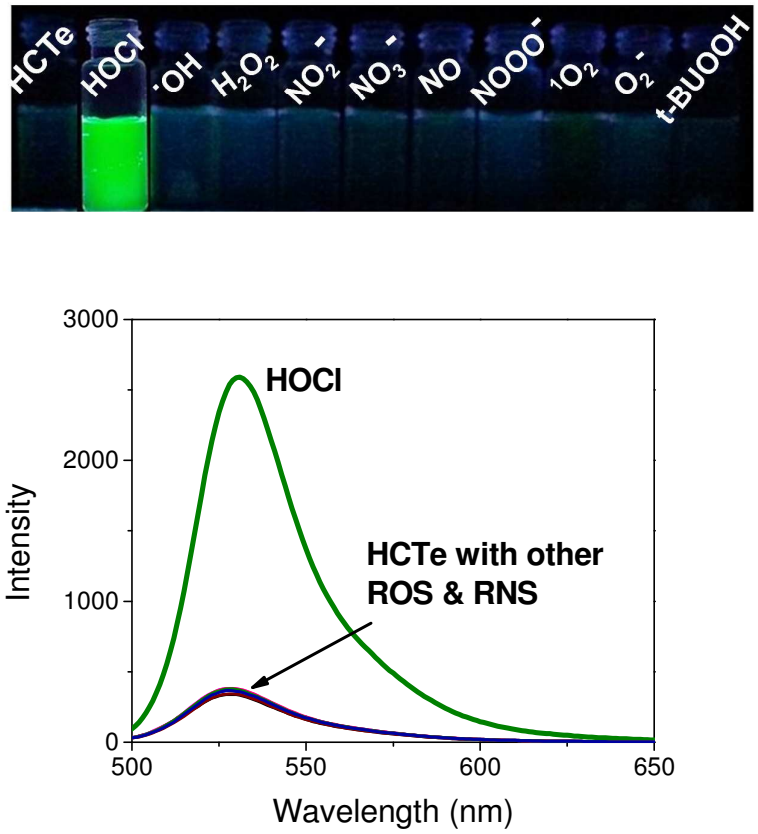


**Fig. 1.** Fluorescence response of **HCTe** (10 μM) toward HOCl and other ROS and RNS (100 μM) in $H_2O$-$CH_3OH$ (v/v = 99/1, 0.1 M PBS, pH 7.4). The excitation wavelength was 480 nm.

Analyst Accepted Manuscript

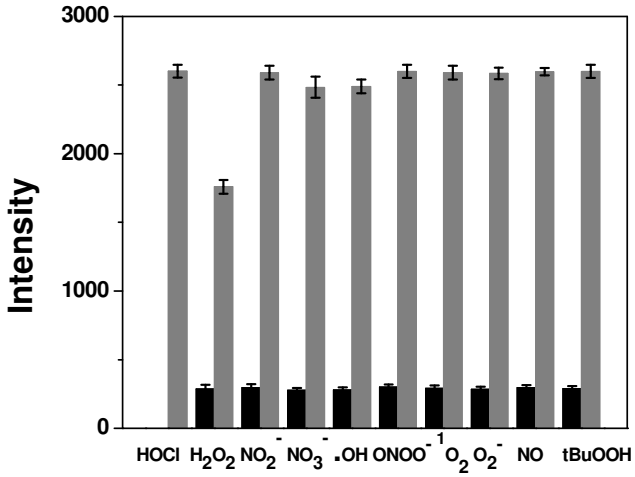


**Fig 2**. Fluorescence changes (530 nm) of probe **HCTe** (10 μM) to NaOCl (15 μM) or 100 μM of other ROS/RNS (the black bar portion) and to the mixture of other ROS/RNS (100 μM) with 15 μM of NaOCl (the red bar portion) in a water– $CH_3OH$ solution (v/v = 99/1, 0.1 M PBS, pH 7.4). The excitation wavelength was 480 nm.

Analyst Accepted Manuscript

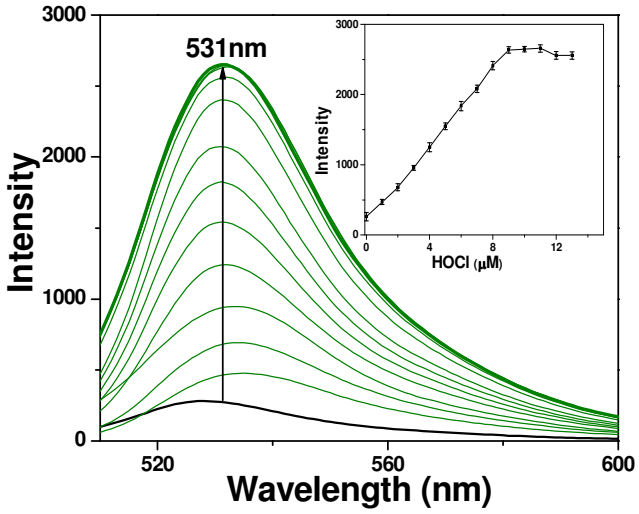


**Fig. 3.** Fluorescence changes of HCTe (10 μM) in the presence of various equivalents of NaOCl in a $H_2O$-$CH_3OH$ (v/v = 99/1, 0.1 M PBS, pH 7.4) solution. The excitation wavelength was 480 nm.

Analyst Accepted Manuscript

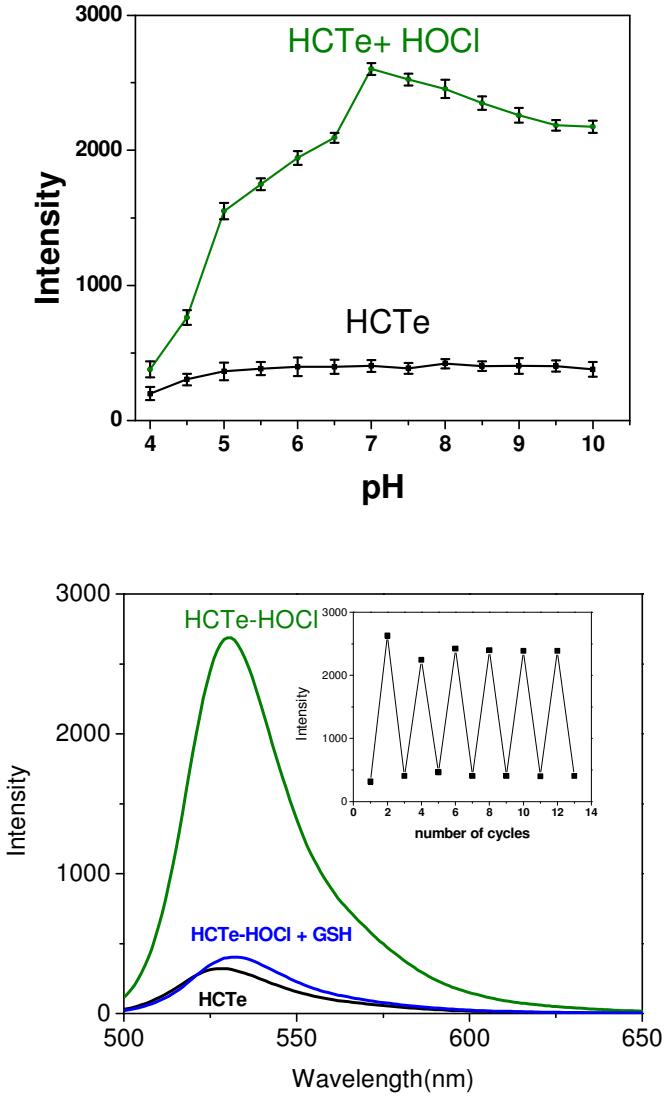


**Fig. 4.** (top) Fluorescence response (530 nm) of free probe **HCTe** (10 μM), and after addition of NaOCl (10 μM) to a $H_2O$–$CH_3OH$ solution (v/v = 99/1) different pH values. (bottom) Reversibility of the interaction between **HCTe** (10 μM) and NaOCl (10 μM) by the introduction of GSH to the system in a $H_2O$-$CH_3OH$ (v/v = 99/1, 0.1 M PBS, pH 7.4) solution.

Analyst Accepted Manuscript

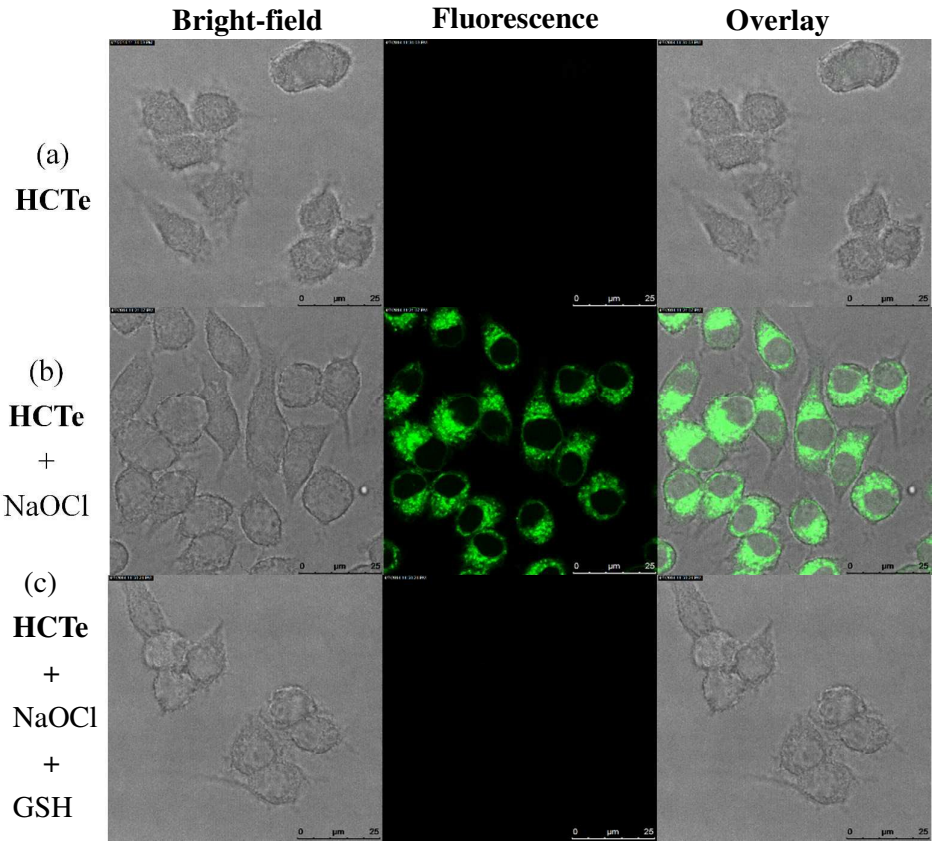


**Fig. 5**. Fluorescence images of RAW264.7 cells. (Left) Bright field image; (Middle) fluorescence image; and (Right) merged image. (a) The cells incubated with **HCTe** (10 μM) for 30 min. (b) Subsequent treatment of the cells with NaOCl (10 μM) for 10 min. (c) Further incubation with GSH (200 μM) for 30 min.

Analyst Accepted Manuscript

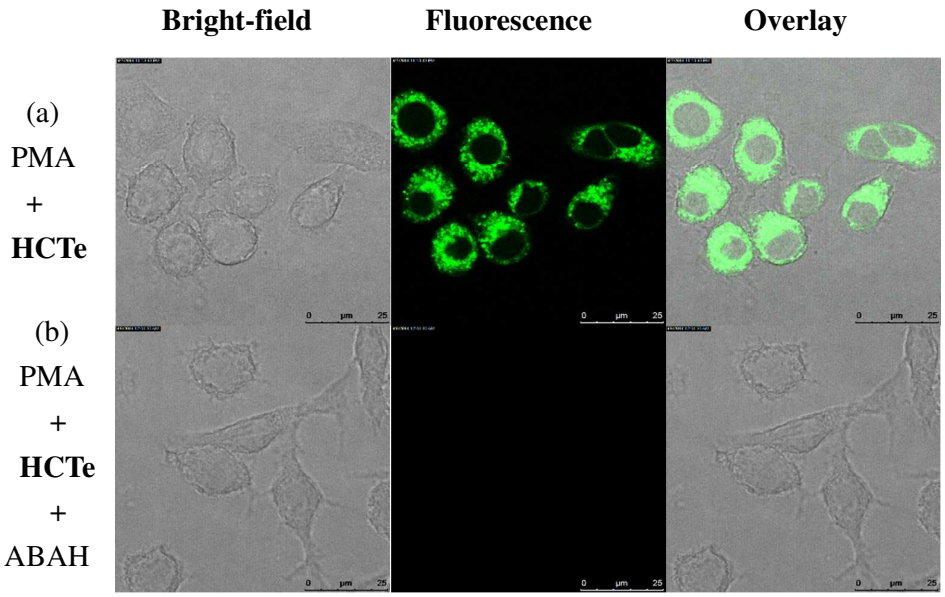


**Fig. 6.** Detection of PMA-induced HOCl production in RAW264.7 cells. (a) The cells treated with PMA (25 ng/mL) for 2 h at 37 °C in the presence of **HCTe** (10 μM). (b) ABAH (100 μM) was co-incubated with **HCTe** (10 μM) for 1 h at 37 °C during PMA stimulation.

Analyst Accepted Manuscript